Spontaneous and Thermally Induced Self-Organization of A−B−A Stereoblock Polymers of *N*-Isopropylacrylamide in Aqueous Solutions

Markus Nuopponen, Katriina Kalliomäki, Vladimir Aseyev, and Heikki Tenhu*

Laboratory of Polymer Chemistry, Department of Chemistry, University of Helsinki, PB 55, FIN-00014 HY, Finland

Received January 12, 2008; Revised Manuscript Received April 30, 2008

ABSTRACT: Well defined A−B−A stereoblock polymers with atactic poly(*N*-isopropylacrylamide) as a hydrophilic block (either A or B) and a water-insoluble block consisting of isotactic poly(*N*-isopropylacrylamide) were dispersed in water to form, depending on the chain composition, spontaneously micelles of different morphologies. The structures of the A−B−A stereoblock polymers were carefully characterized using light scattering methods, microcalorimetry, and turbidity. The self-organization and thermally induced phase separation of the stereoblock polymers is strongly affected by the block sequence but not notably affected by thermal history of the polymer solutions. Both flower-like and coil-like branched micelles were observed. Thermal behavior of these is different. However, all polymers form colloidally stable aggregates at elevated temperatures.

Introduction

Block copolymers have raised an increasing interest due to their unique self-assembly properties as a consequence of their molecular structure.[1] Self-assembling of block copolymers in dilute or semidilute solutions provides a versatile mechanism for the creation of multiple morphologies.[2–4] In dilute solutions, block copolymers form fascinating colloidal aggregates such as polymeric nanoparticles, micelles,[5] or vesicles.[6]

Poly(*N*-isopropylacrylamide) (PNIPAM)[7,8] is one of the most extensively investigated synthetic water-soluble temperature-responsive polymers, attracting great interest as a basic building block of smart materials.[9] This polymer is soluble in water below 32 °C. When temperature is raised above the demixing temperature 32 °C, the hydrophobic backbone and isopropyl groups of the polymer tend to associate. This causes intra- and intermolecular aggregation leading to the collapse of the PNIPAM chains. This temperature is also known as the cloud point because the warm solutions look cloudy, which generally is understood as microscopic phase separation.

Controlled radical polymerization techniques have provided a new set of tools to prepare polymeric building blocks.[10] These methods emerged in the mid-1990s, and since then these techniques have been intensively studied as they combine simplicity of conventional radical polymerization and living character of anionic polymerization. Due to the progress in the controlled radical polymerization, it is relatively easy to synthesize block copolymers consisting of blocks with different responsive characters (e.g., temperature and pH sensitive blocks).[11,12] Thermoresponsive behavior of PNIPAM in aqueous solution can be modified by copolymerization with other monomers and by changing the block order.[13,14] Various linear PNIPAM block copolymer architectures, such as ABA,[15–18] ABC triblocks,[19] multiblock copolymers,[20,21] or telechelic hydrophobically modified PNIPAMs,[22–24] have been shown to produce different morphologies.

Simultaneous control of stereo regularity and molecular weight distribution is one of the novelties in radical polymerization. The stereochemical control in radical polymerization has been considered more difficult compared to ionic or coordinative polymerizations. Recently, there have been reports of simultaneous tacticity and molecular weight control with certain monomers in radical polymerizations.[25] Reversible addition fragmentation chain transfer (RAFT) polymerizations carried out in the presence of Lewis acids have been one of the most successful ways to achieve tacticity control in controlled radical polymerization.[26] RAFT polymerization of NIPAM in the presence of Lewis acid has been reported by Ray et al.[27,28] It was observed that the water solubility of PNIPAM strongly depends on the stereoregularity. Ray et al. demonstrated that the phase transition temperature gradually decreased with an increase in the degree of isotacticity of the PNIPAM.[29] The stereoregularity of the PNIPAM was widely varied from isotactic to syndiotactic in living anionic polymerization by Ito et al.[30] They also showed that the isotactic enough PNIPAM was insoluble in water. In addition, they observed that syndiotacticity increases the water solubility of PNIPAM.

We recently synthesized A−B−A stereoblock polymers of NIPAM, where defined blocks of certain stereoregularity may be prepared from just one monomer.[31] In the present study, we show how isotactic PNIPAM blocks and block order affect the phase-transition and self-organization of PNIPAM in water. A−B−A stereoblock polymers of NIPAM are shown to aggregate in dilute aqueous dispersions forming spontaneously different micelle-like structures depending on their chain composition. Because of their resemblance to many biological systems, the understanding of the mechanism of micelle formation in block copolymer systems is of significant importance. Current work demonstrates the impact of the stereoregularity in the block polymers on the phase transition of the aqueous PNIPAM dispersions.

Experimental Section

Materials. The polymer synthesis was described previously.[31] A−B−A stereoblock polymers with atactic poly(*N*-isopropylacrylamide) as a hydrophilic block (either A or B) and a water-insoluble block consisting of isotactic poly(*N*-isopropylacrylamide) were synthesized using RAFT polymerizations (Table 1). Yttrium trifluoromethanesulfonate was used in the tacticity control and bifunctional *S*,*S*′-bis(α,α′-dimethyl-α″-acetic acid)-trithiocarbonate (BDAT) was utilized as a RAFT agent. Chain structures of the A−B−A stereoblock polymers were determined using ^{1}H NMR, SEC, and MALDI-TOF mass spectrometry. Unfortunately, the overlapping of the meso dyad peak with the racemo peak prevented the exact quantitative determination of

* Corresponding author. E-mail: Heikki.Tenhu@helsinki.fi. Phone: +358-9-19150334. Fax: +358-9-19150330.

10.1021/ma800083t CCC: $40.75
Published on Web 06/04/2008

Table 1. Characteristics of A−B−A Stereoblock Polymers

sample[a]	macroRaFT[b] [M_n (g mol^{-1})]	$M_{n,theo}$	$M_{n,SEC}$	M_w/M_n[c]	ΔH[d] (kJ mol^{-1})
i2−a40−i2	4200	44 200	47 100	1.29	5.5
i2−a28−i2	4200	39 200	36 700	1.29	5.5
a12−i5−a12	24 300	29 300	28 900	1.32	6.4
a12−i10−a12	24 300	34 300	34 500	1.37	6.0

[a] atactic, *i*=isotactic PNIPAM sample/block. [b] a24.3 and i4.2 are MacroRAFT agents used in block polymerizations. [c] M_n and M_w/M_n were determined using SEC with PMMA standards. [d] Heating rate in microcalorimetry (c = 1.0 mg/mL) measurements was 0.5 °C min^{-1}. The enthalpy of phase transition (ΔH) is per repeating monomer unit.

the degree of isotacticity of the polymers. However, isotactic PNIPAM is insoluble in water at room temperature, indicating that racemo content is at least 70%.[29,30] The dispersions of polymeric particles were prepared at room temperature in deionized water (Elgastat UHQ-PS water purification system). Aqueous solutions were passed through the hydrophilic Millex-HV 0.45 μm pore size prior to measurements to remove dust particles.

Light Scattering Experiments. Dynamic light scattering, DLS, and static light scattering, SLS, experiments were conducted with a Brookhaven Instruments BI-200SM goniometer, a BI-TurboCorr digital auto/crosscorrelator, and a BI-CrossCorr detector, including two BI-DS1 detectors. A Sapphire 488−100 CDRH laser from Coherent GmbH operating at the wavelength of λ_o = 488 nm (vertically polarized) and the power adjusting from 10 to 50 mW was the light source. The scattering angles were varied in the range of θ = 30°−150°. Time correlation functions were analyzed with a Laplace inversion program CONTIN. Solutions were equilibrated for 30 min before the measurements. In the DLS experiments, pseudo cross-correlation functions of the scattered light intensity, $G_2(t)$, were collected with the self-beating method, which was used for the determination of the average line width (Γ). The first cumulant, Γ_1, is directly related to the translational diffusion coefficient D or to the hydrodynamic radius R_h

$$R_h = \frac{kT}{6\pi\eta_0\Gamma_1}q^2 \quad (1)$$

where k_B, η, and T are the Boltzmann constant, the solvent viscosity and the absolute temperature, respectively.

In the SLS experiments, the time average intensities of the scattered light, I_θ, were analyzed by means of the Zimm's method. Scattering intensity, where the effect of solvent and scattering angle has been taken into consideration, can be written as $I_\theta = (I_{\theta\ \mathrm{solution}} - I_{\theta\ \mathrm{solvent}})\sin\theta$, with $I_{\theta,\mathrm{solution}}$, $I_{\theta,\mathrm{solvent}}$, θ being the scattering intensity of the solution, scattering intensity of the solvent, and scattering angle, respectively. I_θ has been presented as a function of q^2. Scattering function $P(q)$ is written as $P(q) = I_\theta/I_{\theta=0} = 1 - ((R_g^2q^2)/3)$ where $I_{\theta=0}$ is the estimated extrapolated intensity at zero angle. Thus, $q = (4\pi n_0/\lambda)(\sin(\theta/2))$ is the scattering vector, where n_0 and λ are refractive index of the solvent and the wavelength, respectively.

The temperature of the samples was controlled by means of a Lauda RC 6C thermostatted water bath. The specific refractive index increments (dn/dc) of the PNIPAM stereoblock polymers in water were determined at 20 °C from refractive indices measured by Billingham & Stanley Abbe60/ED refractometer using the same source of incident light as for the LS measurements. The dn/dc for the block polymers was 0.16 mL g^{-1} (λ_o = 488 nm).

Microcalorimetry. High-sensitivity differential scanning calorimetry, HS-DSC, measurements were performed for aqueous polymer dispersions with a VP-DSC microcalorimeter (MicroCal Inc.) under an external pressure of ca. 180 kPa. Concentrations were 0.2, 1.0, 2.0, and 5.0 g L^{-1}. Temperature interval was from 10 to 70 °C and heating rate was 0.5 °C min^{-1}.

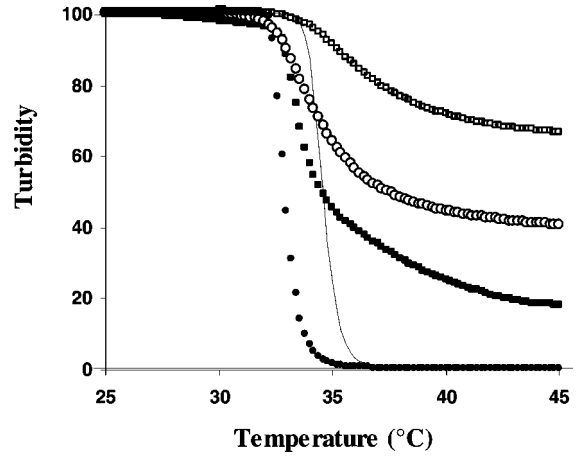

Figure 1. Turbidity of aqueous solutions of PNIPAM polymers i2−a28−i2 (□), i2−a40−i2 (○), a12−i10−a12 (■), a12−i5−a12 (●), and a24.3 (line) measured by UV−vis spectrometry (c = 1.0 g L^{-1}, heating rate = 0.2 °C min^{-1}).

Turbidity Measurements. Turbidity was recorded on a Shimadzu UV-1601PC spectrophotometer at a wavelength of 550 nm. Temperature was varied from 20 to 50 °C with a heating rate of 0.2 °C min^{-1}.

Results and Discussion

Table 1 shows the characteristics of studied PNIPAM A−B−A stereoblock polymers, the details of the syntheses are described elsewhere.[31] In the studied polymers, atactic poly(*N*-isopropylacrylamide) forms the thermoresponsive hydrophilic blocks (either A or B) and the water-insoluble blocks consist of isotactic poly(*N*-isopropylacrylamide). The codes for the polymers are as follows. For example, i2 stands for an isotactic block with M_n approximately 2000 g mol^{-1}, and a28 is an atactic block with M_n about 28 000 g mol^{-1}. From previously introduced polymers, block polymers having short isotactic blocks were selected to be studied further in dilute aqueous dispersions. This selection was because the stereoblock polymers with longer isotactic sequences form gels or do not disperse at all in water at ambient temperature. Those polymers were studied separately in more concentrated solutions.[32]

The stereoblock polymers with short isotactic blocks disperse spontaneously in water, even though isotactic PNIPAM is water-insoluble. Isotactic macroinitiator i4.2.[31] is insoluble in water at studied temperature range (above 0 °C) and was not studied as such. Cloud points of 0.1 wt % aqueous dispersions of polymers were measured by UV−vis spectrometry. Transmittances of the dispersions were recorded with increasing temperature (heating rate = 0.2 °C min^{-1}). Figure 1 shows turbidity vs temperature plot for all four stereoblock polymers and one atactic PNIPAM (a24.3). It should be noted that the cloud point observed for atactic PNIPAM is somewhat high due to hydrophilic carboxylic acid end groups. PNIPAM cloud points are affected by the isotactic blocks. When the isotactic block is a middle one, cloud point temperature decreases compared to atactic PNIPAM. This observation is consistent with that of Ray et al.; isotacticity decreases the cloud point.[29] On the contrary, the effect of the isotactic block is different in block polymers where isotactic blocks are the outer ones. Sharpness of the transition and the shape of the turbidity curve were strongly affected by chain configuration. The transmittances of i2−a28−i2 and i2−a40−i2 dispersions decreased only moderately at elevated temperatures compared to a12−i10−a12 and a12−i5−a12

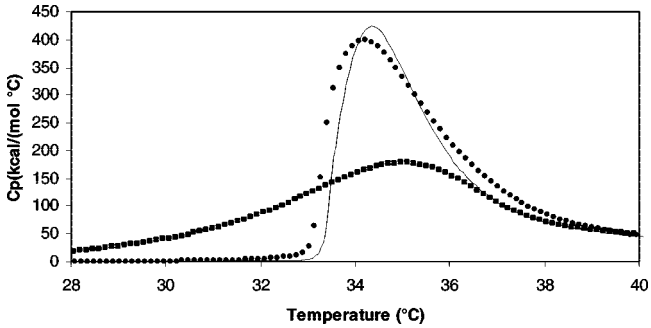

Figure 2. Microcalorimetric endotherms of aqueous solutions of a12−i5−a12 (●), a12−i10−a12 (■), and a24.3 (line) (c = 1.0 g L^{-1}, heating rate = 0.5 °C min^{-1}).

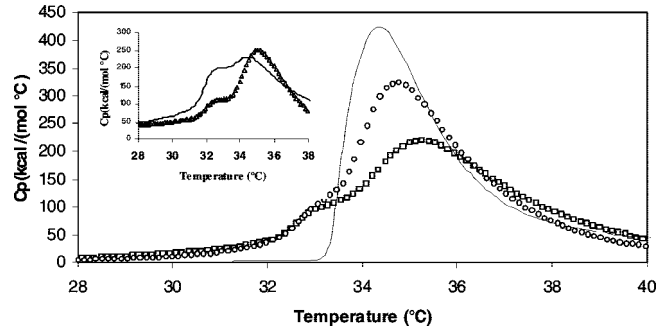

Figure 3. Microcalorimetric endotherms of aqueous solutions of i2−a28−i2 (□), i2−a40−i2 (○), and a24.3 (line) (c = 1.0 g L^{-1}, heating rate = 0.5 °C min^{-1}). Inset shows the endotherms of i2−a2−8i2 in c = 0.2 g L^{-1} (Δ) and c = 5.0 g L^{-1} (line).

particles or atactic PNIPAM, which precipitates out from the solution around 35 °C. The i2−a28−i2 and i2−a40−i2 dispersions showed higher stability upon heating and remained stable after 45 °C. The shape of the turbidity curve of a12−i5−a12 was pretty similar to that of atactic PNIPAM, indicating that a short isotactic middle block functions merely as a hydrophobic modifier. Instead, a12−i10−a12 showed a notably gentler slope, showing that a longer isotactic middle block increases the stability of the PNIPAM particles. However, the influence of the isotactic block on the stability of the polymer dispersions was more evident when the isotactic blocks were the outer ones. Especially, the turbidity of the i2−a28−i2 dispersion decreased only slightly with temperature, this indicating that the polymer dispersion keeps stabile upon heating and PNIPAM does not precipitate out from the solution. It is assumed that these stereo block polymers (apart from a12−i5−a12) form colloidal aggregates/mesoglobules at temperatures above the cloud point where isotactic blocks interact as stabilizing agents.[33]

Next, the phase-transition of the polymer dispersions were investigated by high-sensitivity differential scanning calorimetry (HS-DSC). Figure 2 shows endotherms of a24.3 homo PNIPAM and two stereoblock polymers, a12−i5−a12 and a12−i10−a12, where isotactic block is the middle one. (c = 1.0 g L^{-1}, heating rate = 0.5 °C min^{-1}). Stereoblock polymers have broader phase transitions compared to the atactic PNIPAM,[34] which as we have shown previously, may be due to the PNIPAM chains locked in a hydrophobic environment on the surface of the particles.[35] The endothermic peak width at half-height, $T_{1/2}$, varied from 2.2 °C (homo PNIPAM) to 5.3 °C (a12−i10−a12). The a12−i10−a12 polymer undergoes a broad and continuous phase transition whereas the phase transition of the a12−i5−a12 is very similar to that of a24.3. Thus, microcalorimetry results are consistent with the conclusion based on the turbidity measurements; the shorter isotactic block in the middle of the stereoblock polymer is not long enough to noticeably alter the phase separation behavior. The a12−i5−a12 polymer has only a slightly lower onset temperature of the cloud point compared to atactic PNIPAM.

More interestingly, two endothermic maxima were detected for i2−a28−i2 and i2−a40−i2 (Figure 3). The first transition, $T_{dem} \sim$ 32.8 °C, is equal for both polymers and also concentration independent (inset of Figure 3). We assume that the first transition is the transition from a random coil to an ordered coil.[36] Since water is not a poor solvent below the cloud point, the PNIPAM segments are in a swollen state. As the temperature is increased, isotactic blocks tend to further associate causing the ordered coil state. The second and broader transition corresponds to the intermolecular aggregation of the individual particles and the collapse of the PNIPAM. The collapse temperature of the i2−a28−i2 (T_{dem} = 35.2 °C) is slightly higher compared to i2−a40−i2 (T_{dem} = 35.2 °C) or a24.3 PNIPAM (T_{dem} = 34.6 °C). This observation could be rationalized in the following way. Isotactic outer blocks associate and force stereoblock polymers to form looped, flower-like structures. Higher transition temperature reflects the fact that looped PNIPAM chains on the surface of the locked structures have to overcome an additional internal stress compared to free PNIPAM chains in solution.[36] Further, the water-insoluble isotactic blocks function as structure making components increasing the stability of the particles at elevated temperatures.[33] On the other hand, the temperature maximum of the second transition decreases with concentration (T_{dem} = 35.3, when c = 0.2 g L^{-1} and T_{dem} = 34.3 °C, when c = 5.0 g L^{-1}). This indicates that the interchain interactions of PNIPAM take place earlier at higher concentration, meaning also that at higher concentration effect of the chain configuration is different. At higher concentrations (90 g L^{-1}), the studied polymers show only one transition peak, form gels, and precipitate above could point temperature.[32] Nojima et al. have also recently studied flower micelles and demonstrated that micellization and gelation, respectively, occur in dilute and concentrated telechelic hydrophobically modified PNIPAM solutions.[37]

Enthalpies of the phase transition (ΔH) per repeating unit for all samples are within the same range and correspond to literature values for PNIPAM,[8,38] The observation is confusing, suggesting that the structure of the hydration layer around isotactic PNIPAM is similar to that around an atactic chain. If this were the case, the reason for the insolubility of isotactic PNIPAM would simply be the rigid structure of the chain. It can be assumed that the isotactic chains (which should adopt a helical conformation) form more intramolecular C═O···H−N hydrogen bonds.[29] As a consequence, isotactic sequences reduce the solubility and the flexibility of the polymers. It has been suggested that in addition to the dehydration of the PNIPAM layer dissociation of intramolecular C═O···H−N hydrogen bonds contributes to the enthalpy change upon the phase transition.[39] We assume that an increased amount of intra- and intermolecular bonds is the reason behind the increased colloidal stability of the stereoblock copolymers, because extra energy is needed to trigger the dissociation of the intramolecular bonds and, thus, phase-separation. This hypothesis is supported by our studies on i4.2. Even if i4.2 is insoluble in water at e.g. room temperature, it slowly dispersed in water at elevated temperature (70 °C). Dispersion was naturally opaque since temperature was above the cloud point. However, dispersibility shows that when intra- and intermolecular hydrogen bonds break up PNIPAM conformation changes. The hydration layer around the PNIPAM is concentration dependent. When concentration is increased, the intramolecular hydrogen bonds gradually start to dominate over the polymer−water H-bonds. Also, the intermolecular hydrogen bonds increase in number, this eventually leading to gelation. Clearly, this matter needs to be carefully studied in future.

Table 2. Characteristics of Stereoblock Polymers Measured by Light Scattering[a]

sample	$\langle R_g \rangle$	$\langle R_h \rangle$	$\langle R_g \rangle / \langle R_h \rangle$	A_2	density (g cm^{-3})	$M_{w,agg}$ (10^6 g mol^{-1})	N^{agg}
i2−a28−i2	25	29	0.86	2.2×10^{-4}	0.011	0.82	26
i2−a40−i2	26	21	1.23	9.7×10^{-4}	0.015	0.51	15

[a] Light scattering measurements were performed at 20 °C, the hydrodynamic radii ($\langle R_h \rangle$) were measured by DLS. Time correlation functions were analyzed with a Laplace inversion program (CONTIN), dn/dc, refractive index increment. Measurements at several finite angle concentrations by static light scattering were extrapolated in a Zimm plot to determine $\langle R_g \rangle$, $\langle R_g \rangle / \langle R_h \rangle$, M_w of aggregates ($M_{w,agg}$), aggregation number (N_{agg}), second virial coefficient (A_2), and density of the aggregates calculated using $\langle R_h \rangle$.

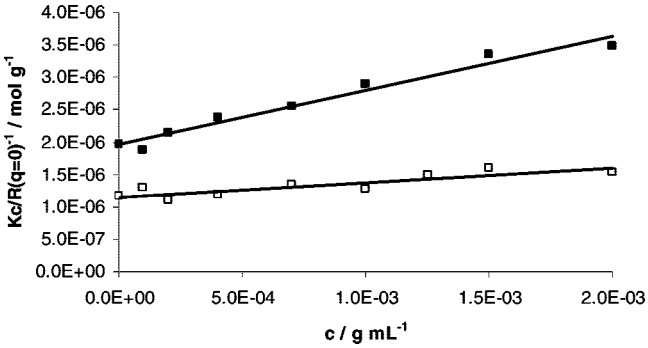

Figure 4. Scattering intensity at zero angle plotted as a function of polymer concentration at 20 °C for i2−a28−i2(□) and a12−i10−a12(■).

The polymer dispersions of a12−i10−a12 and i2−a28−i2 were further studied by static and dynamic light scattering. The purpose was to evaluate the effect of block sequence and, thus, to compare i2−a28−i2 and a12−i5−a12, because these polymers have almost equal atactic and isotactic block contents. However, on the basis of turbidity and microcalorimetry measurements, it was already clear that the polymers behave differently and a12−i5−a12 do not form aggregates in water at ambient temperature. Thus, we selected a12−i10−a12 and i2−a28−i2 for comparison, because the total molar masses of the polymers are similar. Also, based on turbidity and microcalorimetry measurements, i2−a28−i2 forms more stable dispersions than i2−a40−i2 and was more interesting object for light scattering studies. Intensity of the scattered light is sensitive to the molar mass and the size of the scatterers as well as to the thermodynamic quality of the solvent. The scatterers observed in the dispersions were too large to represent individual macromolecules at temperatures below and above the critical. Mean values of hydrodynamic radius distributions, R_h, suggest that below the cloud point polymers form small aggregates. Light scattering data obtained on several scattering angles and concentrations were treated with Zimm double extrapolation which permits the determination of single aggregate properties such as the molar mass of the aggregates ($M_{w,agg}$), aggregation number (N_{agg}), radius of gyration ($\langle R_g \rangle$), density ($\langle \rho \rangle$), and the second virial coefficient (A_2) (Table 2, Figure 4). Hydrodynamic radii ($\langle R_h \rangle$) of both polymer aggregates were small, and the size distribution at 20 °C was unimodal, though broad, which is typical to PNIPAM.[40] It is worth mentioning that we did not detect a critical aggregation concentration (cac) for either polymer in the studied concentration range (0.1−5.0 g L^{-1}). The average hydrodynamic radii ($\langle R_h \rangle$) were independent of the initial polymer concentration and were not affected by dilution, indicating that aggregates reach a certain equilibrium state where structures build up spontaneously, depending on the block sequence. No angular dependence was found within the experimental error.

Scheme 1. Schematic Picture of Flower-Like i2−a28−i2 (Left) and Branched a12−i10−a12 (Right) Micelles

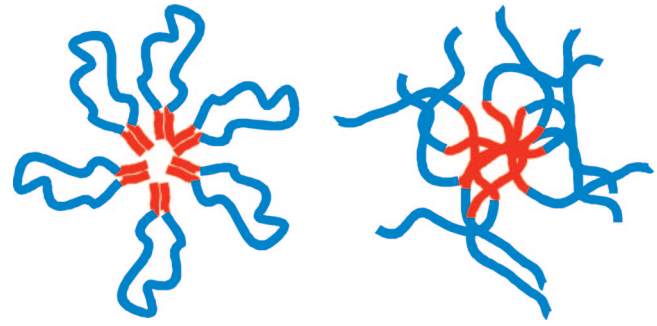

$\langle R_g \rangle$ and N_{agg} of i2−a28−i2 were 25 nm and 26, respectively. For a12−i10−a12, $<R_g>$ = 26 nm and N_{agg} = 15. However, $\langle R_h \rangle$ and thus $\langle R_g \rangle / \langle R_h \rangle$ values are indicative of very different structures of the scattering objects. $\langle R_g \rangle / \langle R_h \rangle$ = 0.86 for i2−a28−i2 indicates a uniform spherical micelle structure, whereas a12−i10−a12 having $\langle R_g \rangle / \langle R_h \rangle$ = 1.23 can be judged to be a more coil-like, branched micelle.[41] The densities of the aggregates are much smaller than those predicted for dense globules indicating as well that aggregates form coil-like structures at ambient temperature and contain a lot of water inside their hydrodynamic volume.[34,42] Furthermore, we compared the second virial coefficients (A_2) of the aggregates: $A_2 = 2.2 \times 10^{-4}$ mol mL g^{-2} for i2−a28−i2 and $A_2 = 9.7 \times 10^{-4}$ mol mL g^{-2} for a12−i10−a12. The positive and small values of A_2 indicate that water is a selective solvent for both polymers.[43] The higher A_2 for a12−i10−a12 particles shows

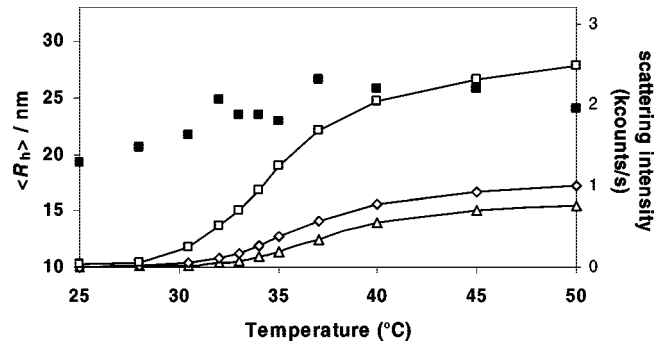

Figure 5. Hydrodynamic radius of a12−i10−a12 (c = 1.0 g L^{-1}) by dynamic light scattering (■). Cloud point slightly decreases as concentration increases: c = 0.2 m L^{-1} (Δ), c = 1.0 m L^{-1} (◇), C = 2.0 g L^{-1} (□). Size distribution kept monomodal throughout the whole temperature range.

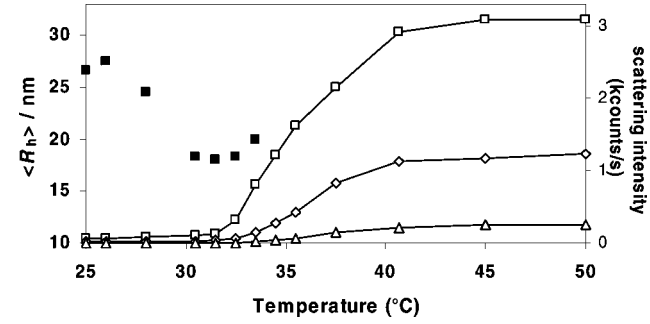

Figure 6. Hydrodynamic radius of i2−a28−i2 (c = 1.0 g L^{-1}) by dynamic light scattering (■). Cloud point slightly decreases as concentration increases: c = 0.2 g L^{-1} (Δ), c = 1.0 g L^{-1} (◇), c = 2.0 g L^{-1} (□). Above 34 °C a bimodal size distribution of the particles was observed and, thus, these points are not shown. (see also Figure 7)

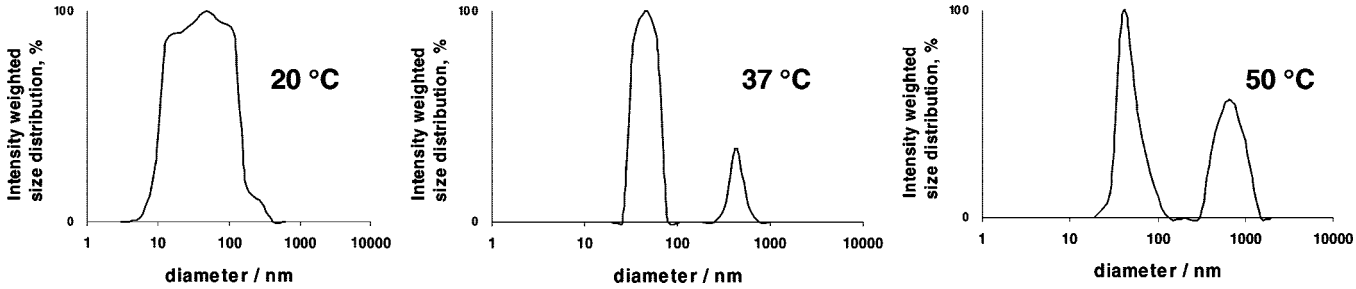

Figure 7. Size distribution of i2−a28−i2 (c = 1.0 g L^{-1}) particles and the dependence of hydrodynamic diameter on temperature.

that the a12−i10−a12 aggregates are more hydrophilic than those of i2−a28−i2. The result might be against expectations, but this can be well understood knowing the different block sequences. Based on light scattering results, we postulate that the stereoblock polymers of PNIPAM reach a certain equilibrium aggregate state where water-insoluble isotactic blocks form a core (Scheme 1). In addition, water-insoluble block is in a glassy state at ambient temperatures[31] stabilizing the formed structures. i2−a28−i2 forms spherical particles where short and stiff isotactic end blocks induce the self-organization and construct the inner core, while atactic blocks keep on the periphery forming loops or rings as the corona of the particles. Also, in the case of a12−i10−a12, the isotactic middle block forms the inner core of the micellar aggregates but the atactic blocks are free to stretch out to the solution, this explaining the more hydrophilic structure.

The thermal transitions of the polymer aggregates were followed by dynamic light scattering (0.2, 1.0, and 2.0 g L^{-1}). Samples were heated slowly and they were allowed to stabilize at each temperature before the measurement. Below the cloud point, intensity and $\langle R_h \rangle$ of the a12−i10−a12 gradually increased upon heating (Figure 5). At the cloud point, scattered light intensity increased sharply. $\langle R_h \rangle$ increases simultaneously indicating the formation of intermolecular aggregates. Diameters of the aggregates reach their maxima around 40 °C and do not change significantly upon further heating. Thus, a12−i10−a12 micelles build up typical multiaggregates upon heating. This kind of formation of colloidally stable PNIPAM mesoglobules has recently been described in literature.[44] Also, other amphiphilic polymers may remain soluble in aqueous medium after the transition to a globular state. Different self-organization of i2−a28−i2 particles was observed. The $\langle R_h \rangle$ of i2−a28−i2 decreased ∼10 nm, when temperature was slowly elevated from 20 to 34 °C, see Figure 6. A moderate decrease means that the motionally restricted looped chains on the corona of the aggregates compressed and the aggregates did not have intermolecular interactions below the cloud point. This compression corresponds to the first transition temperature detected by HS-DSC. Scattering intensity of the particles was concentration dependent and the demixing temperature was slightly lower at higher concentration (Figure 6). Above 34 °C, the aggregate peaks became narrow indicating that dense aggregates/mesoglobules were formed. However, a bimodal size distribution of the particles was observed (Figure 7). The bimodal distribution is caused by the partial aggregation of the particles to multimicelle aggregates. Of course, as is well-known, the number of the bigger scatterers is very low. A−B−A type amphiphilic polymers with nonwater-soluble stickers are known to form flower-like micelles. In addition, amphiphiles may undergo bridging where a network of flowers is connected by bridges.[45,46] We suppose that in the case of i2−a28−i2 some of the micelles are connected in this way. This kind of system can phase separate into two macrophases, one of them being a phase of collapsed network (large diameter) and the other a phase of collapsed invididual aggregates (unchanged diameter). Merging of the aggregate particles requires the reformation of the chains in a way similar to reorganization of hydrophobically modified telechelic PNIPAM chains upon heating.[24] Increasing interactions and the dissociation of the intramolecular C═O···H−N hydrogen bonds can force some particles to reorganize and a temperature responsive morphological transition takes place, upon which small particles fuse to bigger ones.[47] In addition, if the density of the PNIPAM chains in the particle shell is low enough, the atactic PNIPAM remains swollen and retains its capability to sterically stabilize the particles.[48] Once formed, a12−i10−a12 and i2−a28−i2 mesoglobules are very stable at elevated temperatures even for prolonged time (weeks).

The temperature-induced transitions of the studied particles are completely reversible. Upon cooling back to the ambient temperature, the original morphologies are observed again. In addition, the formation of aggregate particles is independent of the thermal history of the samples. It is worth mentioning that even if the particle sizes were not temperature dependent at temperatures below cloud point, the scattering intensity doubled upon heating from 5 to 25 °C (still not comparable to the 2 orders of magnitude increase in scattering at the demixing temperature, Figures 6 and 7). One should also note that even though the thermally-induced self-organization at slow heating rates depends on the block sequence fast-heating protocol provides small mesoglobules typical for linear thermoresponsive polymers.[44] When an aqueous solution of i2−a28−i2 was quickly brought above T_{dem} (nonequilibrium heating) mesoglobules were formed (N_{agg} = 192, A_2 is practically zero, $\langle R_g \rangle$ = 18 nm, $\langle R_h \rangle$ = 26 nm, and thus $\langle R_g \rangle / \langle R_h \rangle$ = 0.71 and density $\langle \rho \rangle$ = 0.21 g/cm^3).

This work displayed a new type of temperature responsive polymer particles based on the self-organization of PNIPAM stereoblock polymers. The present work is a new aspect in the fundamental studies considering PNIPAM self-organization and especially stereoregular PNIPAM polymers. The study adds to the discussion about the effect of chemical composition and stereochemistry on the phase transition of PNIPAM.[49] The findings may be useful in designing new thermosensitive, biomimetic structures by stereocontrolled PNIPAM block polymers.

Conclusions

This study introduced novel PNIPAM stereoblock polymers and discussed the effect of chain configuration on properties of aqueous solutions. When dispersed in water, the block polymers form spontaneously, depending on the chain composition, the branched micelle structures or spherical flower-like micelles. The self-organization and thermally-induced collapse of the stereoblock polymers are strongly affected by the block sequence, as the isotactic blocks notably increase the stability of the particles. Both intra- and intermolecular hydrogen bonds in and between the isotactic blocks are assumed to further strengthen the particles. Especially i2−a28−i2 stereoblock

polymers reorganize even at elevated temperatures, which may also be of interest when constructing vehicles for the delivery of various active substances. Results suggest that the stereoblock polymers of PNIPAM may be useful in the design of various stable thermoresponsive morphologies.

Acknowledgment. The work was supported by ESPOM Graduate School (Electrochemical Science and Technology of Polymers and Membranes including Biomembranes) and Orion-Farmos foundation.

References and Notes

(1) Lodge, T. P. *Macromol. Chem. Phys.* **2003**, *204*, 265–273.
(2) Zhang, L.; Eisenberg, A. *Science* **1995**, *268*, 1728–1731.
(3) Hamley, I. W. *Soft Matter* **2005**, *1*, 36–43.
(4) Cui, H.; Chen, Z.; Zhong, S.; Wooley, K. L.; Pochan, D. J. *Science* **2007**, *317*, 647–650.
(5) Gohy, J. F. *Adv. Polym. Sci.* **2005**, *190*, 65–136.
(6) Antonietti, M.; Foerster, S. *Adv. Mater.* **2003**, *15*, 1323–1333.
(7) Winnik, F. M. *Macromolecules* **1990**, *23*, 233–242.
(8) Schild, H. G. *Prog. Polym. Sci.* **1992**, *17*, 163–249.
(9) Rzaev, Z. M. O.; Dincer, S.; Piskin, E. *Prog. Polym. Sci.* **2007**, *32*, 534–595.
(10) Braunecker, W. A.; Matyjaszewski, K. *Prog. Polym. Sci.* **2007**, *32*, 93–146.
(11) Mertoglu, M.; Garnier, S.; Laschewsky, A.; Skrabania, K.; Storsberg, J. *Polymer* **2005**, *46*, 7726–7740.
(12) Lutz, J. F. *Polym. Int.* **2006**, *55*, 979–993.
(13) Schilli, C. M.; Zhang, M.; Rizzardo, E.; Thang, S. H.; Chong, Y. K.; Edwards, K.; Karlsson, G.; Mueller, A. H. E. *Macromolecules* **2004**, *37*, 7861–7866.
(14) Chen, G.; Hoffman, A. S. *Nature* **1995**, *373*, 49–52.
(15) Convertine, A. J.; Lokitz, B. S.; Vasileva, Y.; Myrick, L. J.; Scales, C. W.; Lowe, A. B.; McCormick, C. L. *Macromolecules* **2006**, *39*, 1724–1730.
(16) Zhou, X.; Ye, X.; Zhang, G. *J. Phys. Chem. B* **2007**, *111*, 5111–5115.
(17) Zhou, J.; Wang, L.; Yang, Q.; Liu, Q.; Yu, H.; Zhao, Z. *J. Phys. Chem. B* **2007**, *111*, 5573–5580.
(18) Zhao, X.; Liu, W.; Chen, D.; Lin, X.; Lu, W. W. *Macromol. Chem. Phys.* **2007**, *208*, 1773–1781.
(19) Li, C.; Buurma, N. J.; Haq, I.; Turner, C.; Armes, S. P.; Castelletto, V.; Hamley, I. W.; Lewis, A. L. *Langmuir* **2005**, *21*, 11026–11033.
(20) Zhou, Y.; Jiang, K.; Song, Q.; Liu, S. *Langmuir* **2007**, *23*, 13076–13084.
(21) Zhang, Q.; Ye, J.; Lu, Y.; Nie, T.; Xie, D.; Song, Q.; Chen, H.; Zhang, G.; Tang, Y.; Wu, C.; Xie, Z. *Macromolecules* **2008**, *41*, 2228–2234.
(22) Kujawa, P.; Watanabe, H.; Tanaka, F.; Winnik, F. M. *Eur. Phys. J. E* **2005**, *17*, 129–137.
(23) Kujawa, P.; Segui, F.; Shaban, S.; Diab, C.; Okada, Y.; Tanaka, F.; Winnik, F. M. *Macromolecules* **2006**, *39*, 341–348.
(24) Kujawa, P.; Tanaka, F.; Winnik, F. M. *Macromolecules* **2006**, *39*, 3048–3055.
(25) Kamigaito, M.; Satoh, K. *Macromolecules* **2008**, *41*, 269–276.
(26) Chong, Y. K.; Moad, G.; Rizzardo, E.; Skidmore, M. A.; Thang, S. H. *Macromolecules* **2007**, *40*, 9262–9271.
(27) Ray, B.; Isobe, Y.; Morioka, K.; Habaue, S.; Okamoto, Y.; Kamigaito, M.; Sawamoto, M. *Macromolecules* **2003**, *36*, 543–545.
(28) Ray, B.; Isobe, Y.; Matsumoto, K.; Habaue, S.; Okamoto, Y.; Kamigaito, M.; Sawamoto, M. *Macromolecules* **2004**, *37*, 1702–1710.
(29) Ray, B.; Okamoto, Y.; Kamigaito, N.; Sawamoto, M.; Seno, K.; Kanaoka, S.; Aoshima, S. *Polym. J.* **2005**, *37*, 234–237.
(30) Ito, M.; Ishizone, T. *J. Polym. Sci., Part A: Polym. Chem.* **2006**, *44*, 4832–4845.
(31) Nuopponen, M.; Kalliomaki, K.; Laukkanen, A.; Hietala, S.; Tenhu, H. *J. Polym. Sci., Part A: Polym. Chem.* **2008**, *46*, 38–46.
(32) Hietala, S.; Nuopponen, M.; Kalliomaki, K.; Tenhu, H. *Macromolecules* **2008**, *41*, 2627–2631.
(33) Zhang, G. Z.; Wu, C. *Adv. Polym. Sci.* **2006**, *195*, 101–176.
(34) Wu, C.; Wang, X. *Phys. Rev. Lett.* **1998**, *80*, 4092–4094.
(35) Nuopponen, M.; Ojala, J.; Tenhu, H. *Polymer* **2004**, *45*, 3643–3650.
(36) Zhang, G.; Winnik, F. M.; Wu, C. *Phys. Rev. Lett.* **2003**, *90*, 035506/1–035506/4.
(37) Nojima, R.; Sato, T.; Qiu, X.; Winnik, F. M. *Macromolecules* **2008**, *41*, 292–294.
(38) Shan, J.; Chen, J.; Nuopponen, M.; Tenhu, H. *Langmuir* **2004**, *20*, 4671–4676.
(39) Katsumoto, Y.; Tanaka, T.; Ihara, K.; Koyama, M.; Ozaki, Y. *J. Phys. Chem. B* **2007**, *111*, 12730–12737.
(40) Virtanen, J. Lemmetyinen, H., Tenhu, H. *Polymer* **2001**, *42*, 9487–9493.
(41) Burchard, W. In Light Scattering Principles and Development; Brown, W., Ed.; Claredon Press: Oxford, 1996, p 439.
(42) Marchetti, M.; Prager, S.; Cussler, E. L. *Macromolecules* **1990**, *23*, 3445–3450.
(43) Zhang, W.; Zhou, X.; Li, H.; Fang, Y.; Zhang, G. *Macromolecules* **2005**, *38*, 909–914.
(44) Aseyev, V. O.; Tenhu, H.; Winnik, F. M. *Adv. Polym. Sci.* **2006**, *196*, 1–85.
(45) Semenov, A. N.; Joanny, J.; Khokhlov, A. R. *Macromolecules* **1995**, *28*, 1066–1075.
(46) Borisov, O. V.; Halperin, A. *Macromolecules* **1996**, *29*, 2612–2617.
(47) Zhou, Y.; Yan, D.; Dong, W.; Tian, Y. *J. Phys. Chem. B* **2007**, *111*, 1262–1270.
(48) Zhu, X.; Yan, C.; Winnik, F. M.; Leckband, D. *Langmuir* **2007**, *23*, 162–169.
(49) Qiu, X.; Tanaka, F.; Winnik, F. M. *Macromolecules* **2007**, *40*, 7069–7071.

MA800083T